ELECTRON PARAMAGNETIC RESONANCE DETERMINATION OF A LOW-LYING EXCITED STATE IN *CHROMATIUM VINOSUM* HIGH-POTENTIAL IRON PROTEIN

HAYWOOD BLUM, J. C. SALERNO, ROGER C. PRINCE, J. S. LEIGH, JR., AND TOMOKO OHNISHI, *Johnson Research Foundation, Department of Biochemistry and Biophysics, University of Pennsylvania, Philadelphia, Pennsylvania 19174 U.S.A.*

ABSTRACT The temperature dependence of the EPR spectrum of oxidized high-potential iron protein from *Chromatium vinosum* has been studied. From line width and intensity measurements it is possible to determine the position of the first excited unoccupied state, 160 ± 10 cm^{-1} above the ground state orbital.

INTRODUCTION

The four-Fe high-potential iron protein (HiPIP) from *Chromatium vinosum* has been well characterized (1, 2). The low-temperature electron paramagnetic resonance (EPR) spectrum has been reported (3, 4) for the oxidized protein, the reduced state being diamagnetic at low temperatures (5).

In experimental (6) and theoretical (7, 8) studies of analogues, molecular orbital calculations were employed to describe the electronic structure. These calculations suggest that the highest occupied orbital lies a few hundred wave numbers below the nearest unoccupied orbital in the reduced form. A molecular orbital calculation has been applied (9) to a description of the EPR spectrum.

Mossbauer (10) and proton magnetic resonance (11) results indicate that the four iron atoms are magnetically inequivalent, suggesting that a straightforward, antiferromagnetically exchange-coupled Gibson model (12, 13) might profitably be employed to describe the HiPIP electronic structure and its magnetic properties.

This model, successful in describing binuclear iron-sulfur clusters, is easily extended to four-iron systems. In the oxidized state, the formal valences of the irons are +3, +3, +3, and +2, with high spin values 5/2, 5/2, 5/2, and 4/2, respectively. In the reduced state, one of the ferric ions is reduced to ferrous and the spin values become 5/2, 5/2, 4/2, and 4/2. With antiferromagnetic exchange, the ground state should have a net spin of $\frac{1}{2}$ or 0 for the oxidized and reduced forms, respectively.

Furthermore, the exchange coupling adds a term to the Hamiltonian of the form $-2\sum_{ij} S_i \cdot S_j$, where J_{ij} is the exchange coupling constant between spin i and spin j ($J_{ij} < 0$ for antiferromagnetic coupling). From this we can predict a set of excited

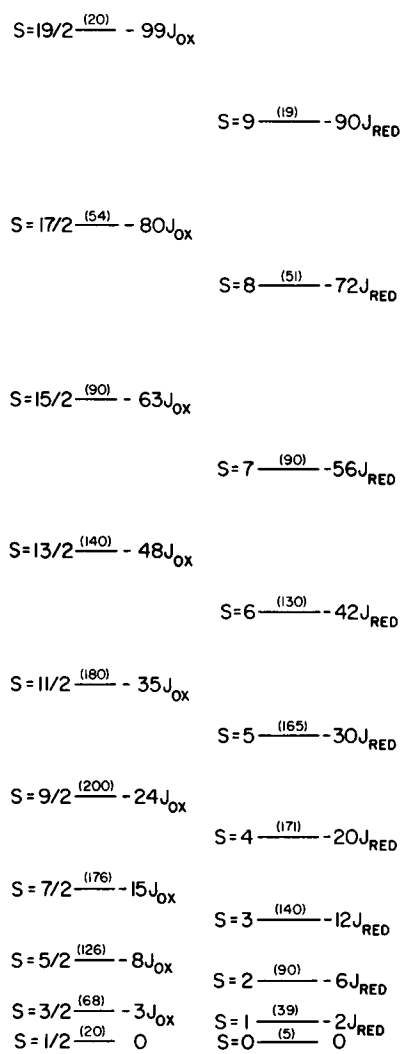

FIGURE 1 Set of states calculated under the assumption of a single exchange coupling constant. The spin and energy of each level is given. Numbers in parentheses are total multiplicity. Left, HiPIP oxidized; right, HiPIP reduced.

states (14, 15) which, if they are thermally accessible, will contribute to the magnetic properties of the center (16).

The simplest case will occur if all the J_{ij} are equal. The expected ladder of states derived under this assumption is shown in Fig. 1. The total multiplicity of the individual spin states is given in parentheses.

It is expected that the EPR spectra will reflect the presence of low-lying excited states in two ways. At low temperatures ($kT \ll \Delta$, where Δ is the energy of the excited state), only the ground state will be significantly populated but the first excited state

will become accessible as the temperature is raised. The ratio of populations in the ground state, 0, and first excited state, 1, is given by the Boltzmann factor $N(1)/N(0) = m \exp(-\Delta kT)$, where m is the ratio of multiplicities. It is expected that the excited state will be unobservable via EPR due to its short lifetime. Nevertheless, the decrease in the ground state EPR intensity can be monitored and, from the above discussion, should go as

$$I(0) = I_0(0) \cdot (1 + me^{-\Delta/kT})^{-1}, \tag{1}$$

where I_0 (0) is the predicted intensity, taking into account the simple fall-off in intensity with temperature from the Curie law dependence predicted by the Boltzmann distribution between the ground state Zeeman levels. That is, we predict

$$I(0) \cdot T = I_{LT}(0) \cdot T_{LT} \cdot (1 + me^{-\Delta/kT})^{-1}, \tag{2}$$

where I_{LT} (0) is the low-temperature EPR intensity of the ground state and T_{LT} is the absolute temperature at which $I_{LT}(0)$ is measured.

A second effect of the presence of low-lying excited states on the EPR spectrum can operate through the spin-lattice relaxation time, T_1. If the excited states are more tightly coupled to the vibrational states of the molecule, T_1 for the ground state will decrease as the excited state becomes accessible. This Orbach or resonant Raman process (17,18) has been employed previously to extract the exchange coupling in heme (19) and iron-sulfur proteins (20,21). T_1 can be measured directly or followed indirectly by observation of power saturation or line width.

The line width, δ, given by the Orbach process is (19,20)

$$\delta \propto T_1^{-1} \propto A(e^{\Delta/kT} - 1)^{-1}, \tag{3}$$

which for $\Delta/kT \gg 1$ is

$$\delta \propto Ae^{-\Delta/kT}. \tag{4}$$

The lowest lying excited states need not be most effective in coupling the lattice to the spin so that the energy difference Δ in Eq. 4 could be different from the Δ in Eq. 2.

In this paper we report measurements of the line width and the EPR intensity. We are able to find mutally consistent values for Δ from these two independent measurements, showing that the lowest excited state is responsible for T_1 and for depopulating the ground state.

METHODS

Apparatus

The EPR measurements were made on a Varian E-4 spectrometer (Varian Associates, Palo Alto, Calif.). Temperature control was obtained by use of a flowing helium cryostat (Air Products LTD-3-110, Air Products & Chemicals, Inc., Allentown, Penn.).

Temperature measurements were made with a calibrated carbon resistor placed below the sample at temperatures below 20°K; above 20°K, thermocouples (Chromel [Hoskins Manufacturing Co., Detroit, Mich.] vs. Au- 0.07% Fe), located below the sample and imbedded in

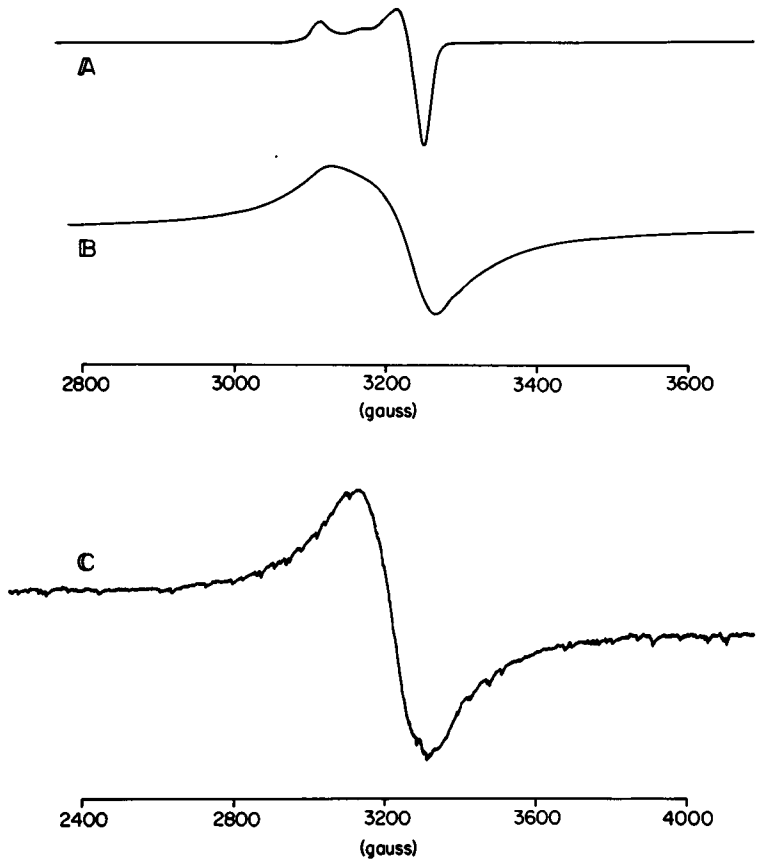

FIGURE 2 Observed EPR absorption derivative signals from oxidized *Chromatium vinosum* HiPIP, solid lines. Temperatures (A) 15°K, (B) 65°K, (C) 78°K. Note change in horizontal scale between (B) and (C). EPR conditions were: microwave power incident on the cavity 2 mW, modulation 10 G(1 mT) at 100 kHz, klystron frequency 9.13 GHz, sweep rate 1,000 G/min (0.1 T/min). Vertical scale is arbitrary.

the sample at the top of the sample tube, were used. Corrections to the measured temperature were made by comparison with the temperature of a thermocouple or carbon resistor placed in the sample location of a blank water-filled sample tube.

Serious errors can occur in the measurement of the EPR intensity if the spectrometer sensitivity fluctuates. The most common problem is changes in the microwave cavity Q caused by changes in dielectric losses with time if ice accumulates in the low-temperature insert. Tests made with an unsaturated Cu-EDTA standard showed that the sensitivity remained stable to within 10% over the temperature range reported here and during the course of a run lasting a few hours. The sensitivity fluctuation from day to day is higher than this, however, and runs made on different days must be scaled appropriately. The sensitivity was also monitored during some of the experiments with similar results by inserting a small diphenylpicryl hydrazyl (DPPH) standard, imbedded in tape, through an optical slit in the microwave cavity. This standard could be removed and reinserted in a reproducible way; it remained at ambient temperature.

Digital integrations were performed with an on-line Nicolet 1074 instrument computer (Nicdet Instrument Corp., Madison, Wis.). At the highest sensitivities the EPR base line invariably deviates from flatness due to cavity resonances and geometrial cavity-modulation effects. Base-line effects on the integration can be obviated by careful application of a linear correction function.

Sample Preparation

C. vinosum strain D was grown anaerobically in the light on a medium containing succinate as the sole carbon source (22). The cells were broken in a French pressure cell, and the chromatophores were removed by centrifugation. HiPIP was prepared from the chromatophore supernatant, essentially by the method of Bartsch (23), using repeated ammonium sulfate precipitation and column chromatography on DEAE cellulose. The HiPIP used in this work was more than 95% pure, and under conditions where HiPIP was oxidized (and EPR-visible), no EPR-detectable contaminants could be resolved. However, in the presence of dithionite, which reduced HiPIP and rendered it EPR-invisible, a small amount ($\sim 1\%$) of a ferredoxin-like g 1.94 iron-sulfur center could be detected. Nevertheless, since all the work reported here involved the oxidized sample, this contaminant did not interfere with the measurements reported here.

RESULTS

Line Width

An interesting feature of the EPR signal is the drastic change from a center with characteristic axial symmetry and Gaussian line shapes at low temperature to an extremely

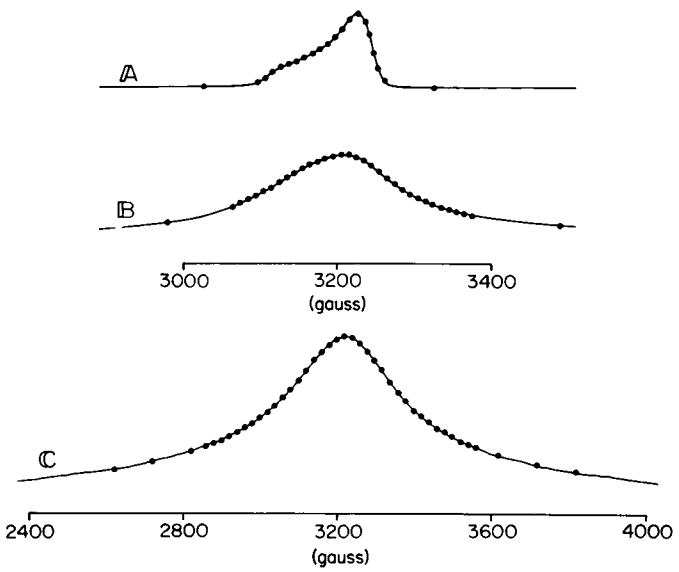

FIGURE 3 Digitally integrated observed EPR absorption signals, solid line. Temperatures as in Fig. 2. Circles are computer-simulated EPR absorption signals. Calculations are described in the text. Individual Lorentzian spin packet half-widths (half-width at half-maximum) (A) 2 G (0.2 MT), (B) 64 G (6.4 mT), (C) 180 G (18 mT). Height of simulated signal adjusted to match observed spectrum at the line center.

broad Lorentzian line at higher temperature (Fig. 2). The signal observed is the convolution of individual homogeneously broadened Lorentzian spin packets with an inhomogeneously broadened Gaussian line shape and the powder pattern axial spectrum (24,25). The analysis of this problem is virtually intractable in closed form (25), but is easily handled numerically.

The low-temperature EPR derivative spectrum was recorded (Fig. 2A) and digitally integrated (Fig. 3A). The digital envelope function was then used to simulate the higher-temperature derivative and absorption spectra. The envelope was numerically convoluted with Lorentzian spin packets of various half-width, in both derivative and absorption form. Since the simulations are derived from the absorption envelope, the simulation of a derivative spectrum is a demanding requirement. Some of the low-field experimental detail is smoothed out, especially in the lower temperature cases, but this is not a significant problem because the derivative spectra are not used in the analysis of the line width. In Fig. 3 the simulated absorption spectra are superimposed on the digitally integrated observed spectra, showing the excellent fit possible.

The procedure employed to determine the appropriate Lorentzian spin packet for each observed EPR spectrum was to construct a correction curve from the simulations, relating the Lorentzian spin packet half-width to the half-width of the resulting envelope. Since the envelopes are asymmetric in general, the half-width is taken as the distance from the peak to the half-intensity point on the high field side. It is not possible to employ the simple relation $\Delta H^2_{obs} = \Delta H^2_{Gaussian} + \Delta H^2_{Lorentzian}$, because of the important effect of the anisotropic g values. In Fig. 4 the observed line half-width

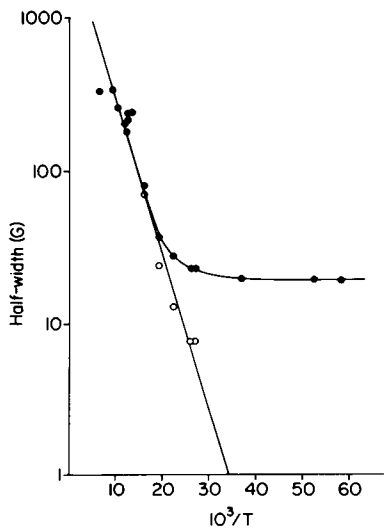

FIGURE 4 Observed EPR half-width versus $10^3/T$, closed circles. Curved line through closed circles is best smooth fit to the data. Open circles are the individual Lorentzian spin packet half-width, δ, extracted from the observed half-width by the method described in the text. For the points above 100 G, δ is equal to the observed value; that is, no correction is necessary. Straight line is least squares fit to data, giving $\Delta = 160 \pm 10\,cm^{-1}$.

defined above is plotted against the inverse temperature. The correct Lorentzian spin packet half-width necessary to achieve the observed half-width is also plotted. The Lorentzian half-width can be represented by the expression $\delta \propto \exp(-\Delta/KT)$, where $\Delta = 160 \pm 10\,\text{cm}^{-1}$.

The line width of the Lorentzian spin packet is inversely related to the spin-lattice relaxation time. The deduced exponential relationship of the relaxation time with temperature implies an Orbach process (Eq. 4), with relaxation mediated by an excited state 160 cm^{-1} above the observed ground state.

Other relaxation forms (18) were tested. It is possible to fit the data over the temperature range studied with a $\delta\alpha\ T^5$ expression suitable for a multilevel ground state in the Raman region (26), but this case does not apply here. More usual T^1 direct process or T^7 and T^9 Raman processes are completely eliminated by the data.

Intensity

The EPR intensity (second integral of the experimentally observed absorption derivative) multiplied by the absolute temperature is plotted in Fig. 5. The curve follows Eq. 2 for $\Delta = 160\ \text{cm}^{-1}$ and $m = 15$. The data have been replotted in Fig. 6 in a

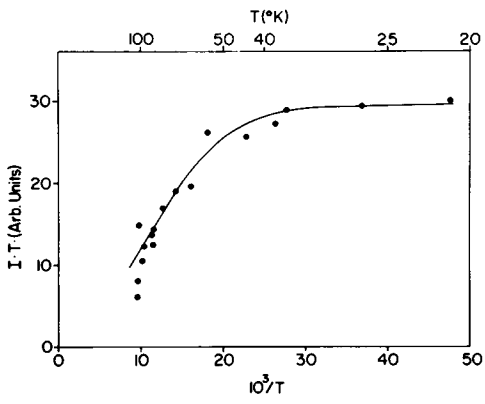

FIGURE 5

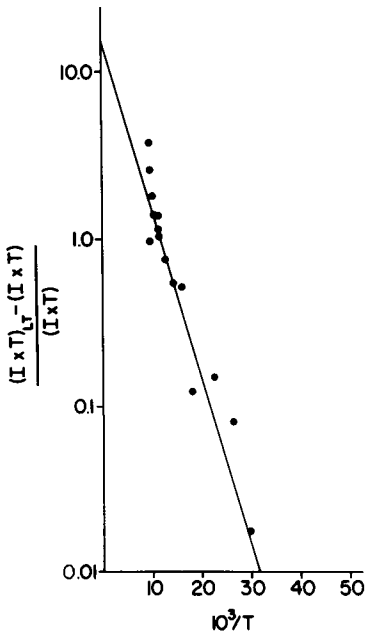

FIGURE 6

FIGURE 5 EPR-integrated intensity multiplied by the absolute temperature versus reciprocal temperature. Circles are data. Curve follows Eq. 2 with $\Delta = 160\ \text{cm}^{-1}$ and $m = 15$.

FIGURE 6 Data of Fig. 5 replotted to show exponential fall-off in intensity with increasing temperature. $(I \times T)_{LT}$ is the low-temperature (<30°K) value of the EPR-integrated intensity multiplied by the absolute temperature. Line is least squares fit to data (circles). Slope of line gives $\Delta = 160 \pm 10\,\text{cm}^{-1}$. Intercept on y-axis gives $m = 15 \pm 5$.

semi-logarithmic form. The line is the best fit to the data; its intercept with the y-axis gives $m = 15 \pm 5$ and its slope gives $\Delta = 160 \pm 10\,cm^{-1}$.

The fit is excellent except at the highest temperatures (above 100°K), where the decrease in intensity is greater than predicted. This might be taken to indicate a higher excited state at approximate $\Delta' = 2{,}000\,cm^{-1}$. However, the data are not good enough to draw a firm conclusion.

DISCUSSION

The results presented above can be interpreted in terms of the anti-ferromagnetic coupling models giving alignment of the electron spins in the tetranuclear iron-sulfur cluster in *Chromatium* HiPIP, with the oxidized form having a paramagnetic $S = 1/2$ ground state and excited state(s) of higher spin. The lowest lying of these is 160 cm^{-1} above the ground state.

The observation that $m = 15$ is puzzling, however. The use of a model analogous to the anti-ferromagnetic coupling model for spinach ferredoxin (12) would predict $m = 3.4$ for oxidized HiPIP; good agreement with this model can be obtained for spinach ferredoxin-type iron-sulfur clusters both by EPR and susceptibility measurements. From molecular orbital models (7,9) one expects values of m of 3 or 9 depending on the particular calculation. This seems to imply that neither model is completely adequate to explain the details of the EPR spectrum of *Chromatium* HiPIP.

More detailed magnetic susceptibility measurements would be of great use in clarifying the situation, but it appears that there are sources of degeneracy other than spin multiplicity in the first excited states of oxidized *Chromatium* HiPIP.

The authors wish to thank Mrs. Heather Bonner for providing skilled technical support.

This research was supported in part by U. S. Public Health Grants GM 12202 and HL-15061-0551 and National Science Foundation Grants BMS 7513459 and PCM 7614209.

Received for publication 29 March 1977 and in revised form 30 May 1977.

REFERENCES

1. CARTER, JR., C. W., J. KRAUT, S. T. FREER, R. A. ALDEN, L. C. SIEHER, E. ADMAN, and L. H. JENSEN. 1972. A comparison of $Fe_4S_4^{\ddagger}$ clusters in high potential iron protein and in ferredoxin. *Proc. Natl. Acad. Sci. U.S.A.* **69**:3526.
2. ORME-JOHNSON, W. H., and R. H. SANDS. 1973. Probing iron sulfur proteins with EPR and ENDOR spectroscopy. *In* Iron Sulfur Proteins, Vol. II. W. Lovenberg, editor. Academic Press, Inc., New York. 195–238.
3. BEINERT, H. 1965. EPR spectroscopy in the detection, study and identification of protein-bound non-heme iron. *In* Non-Heme Iron Proteins: Role in Energy Conversion. A. San Pietro, editor. Antioch Press. 23–42.
4. PALMER, G., H. BRINTZINGER, R. W. ESTABROOK, and R. H. SANDS. 1967. The active centre of non-heme iron proteins. Some recent studies on ferredoxin and andrenodeoxin. *In* Proceedings of the Second International Conference on Magnetic Research in Biological Systems. A. Ehrenberg, B. G. Malmström, and T. Vänngård, editors. Pergamon Press, Inc., Elmsford, N.Y. 159–171.
5. MOSS, T. H., D. PETERING, and G. PALMER. 1969. The magnetic susceptibility of oxidized and reduced ferredoxins from spinach and parsley and the high potential protein from *Chromatium*. *J. Biol. Chem.* **244**:2275.

6. HERSKOVITZ, T., B. A. AVERILL, R. H. HOLM, J. A. IBERS, W. D. PHILLIPS, and J. F. WEIBER. 1972. Structure and properties of a synthetic analogue of bacterial iron-sulfur proteins. *Proc. Natl. Acad. Sci. U.S.A.* **69**:2537.
7. YANG, C. Y., K. H. JOHNSON, R. H. HOLM, and J. G. NORMAN, JR. 1975. Theoretical model for the 4-Fe active sites in oxidized ferredoxin and reduced "high-potential" proteins. Electronic structure of the analogue $[Fe_4S^*(SCH_3)_4]^{2-}$. *J. Am. Chem. Soc.* **97**:6596.
8. AVERILL, B. A., T. HERSKOVITZ, R. H. HOLM and J. A. IBERS. 1973. Synthetic analogs of the active sites of iron-sulfur proteins. II. Synthesis and structure of the tetra [mercapto-μ_3-sulfido-iron] cluster, $[Fe_4S_4(SR)_4]^{2-}$. *J. Am. Chem. Soc.* **95**:3523.
9. THOMSON, A. J. 1975. A model of the tetrahedral iron cluster in iron-sulfur proteins. *Biochem. Soc. Trans.* **3**:468.
10. JOHNSON, C. E., K. K. RAO, R. CAMMACK, M. C. W. EVANS, and D. O. HALL. 1970. Mossbauer studies on iron sulfur proteins. *In* Abstracts, Fourth International Conference on Magnetic Resonance in Biological Systems. The Oxford University Press, London, U.K. 56.
11. PHILLIPS, W. D., M. POE, C. C. MCDONALD, and R. G. BARTSCH. 1970. Proton magnetic resonance study of ferredoxin from *Clostridium pasteurianum*. *Proc. Natl. Acad. Sci. U.S.A.* **65**:797.
12. GIBSON, J. F., D. O. HALL, J. H. M. THORNLEY, and F. R. WHATLEY. 1966. The iron complex in spinach ferredoxin. *Proc. Natl. Acad. Sci. U.S.A.* **56**:987.
13. SANDS, R. H., and W. R. DUNHAM. 1975. Spectroscopic studies on two-iron ferredoxins. *Q. Rev. Biophys.* **7**:443.
14. HUDSON, A. 1971. Nuclear hyperfine interactions in trimeric clusters. *Mol. Phys.* **21**:61.
15. GRUBER, S. J., C. M. HARRIS, and E. SINN. 1968. Metal complexes as ligands. VI. Antiferromagnetic interactions in trinuclear complexes containing similar and dissimilar metals. *J. Chem. Phys.* **49**: 2183.
16. GINSBERG, A. P., M. E. LINES, K. D. KARLIN, S. J. LIPPARD, and F. J. DISALVO. 1976. Orbitally dependent exchange in two sulfur-bridged binuclear iron (II) complexes. II. *J. Am. Chem. Soc.* **98**: 6958.
17. ORBACH, R. 1961. Spin-lattice relaxation in rare-earth salts. *Proc. R. Soc. (Lond.) A.* **264**:458.
18. A. A. MANENKOV and R. ORBACH, editors. 1966. Spin-lattice relaxation in ionic solids. Harper & Row, Publishers, Inc., New York. 453.
19. SCHOLES, C. P., R. A. ISAACSON, and G. FEHER. 1971. Determination of the zero-field splittings of Fe^{3+} in heme proteins from the temperature dependence of the spin-lattice relaxation rate. *Biochim. Biophys. Acta.* **244**:206.
20. GAYDA, J. P., J. F. GIBSON, R. CAMMACK, D. O. HALL, and R. MULLINGER. 1976. Spin-lattice relaxation and exchange interaction in a 2-iron, 2-sulfur protein. *Biochim. Biophys. Acta.* **434**:154.
21. SALERNO, J. C., T. OHNISHI, H. BLUM, and J. S. LEIGH. 1977. Determination of the exchange integral in binuclear iron-sulfur clusters in proteins of varying complexity. *Biochim. Biophys. Acts.* In press.
22. DUTTON, P. L., K. M. PETTY, H. S. BONNER, and S. D. MORSE. 1975. Cytochrome c_2 and reaction center of *Rhodopseudomonas sphaeroides* Ga membranes: extinction coefficients, content, half-reduction potentials, kinetics and electric field alterations. *Biochim. Biophys. Acta.* **387**:536.
23. BARTSCH, R. G. 1971. High potential iron proteins: bacterial. *Methods. Enzymol.*, **23A**:644.
24. POOLE, C. P. 1967. Electron spin resonance. A comprehensive treatise on experimental technique. John Wiley & Sons, Inc., New York. 922.
25. COFFMAN, R. E. 1975. Inhomogeneously broadened line shapes and information content of calculated paramagnetic resonance spectra of biological molecules containing high spin iron (III). *J. Phys. Chem.* **79**:1129.
26. ORBACH, R., and M. BLUME. 1962. Spin-lattice relaxation in multilevel spin systems. *Phys. Rev. Lett.* **8**:478.